

1 **Osmium and Platinum Decoupling in the Environment: Evidences in**
2 **Intertidal Sediments (Tagus Estuary, SW Europe)**

3 *Clara Almécija^{*,†,‡}, Mukul Sharma[‡], Antonio Cobelo-García[†], Juan Santos-Echeandía[†]*
4 *and Miguel Caetano^{§,¶}*

5 [†]Bioxeoquímica Mariña, Instituto de Investigacións Mariñas IIM-CSIC, 36208 Vigo,
6 Spain

7 [‡]Radiogenic Isotope Geochemistry Laboratory, Department of Earth Sciences,
8 Dartmouth College, Hanover, New Hampshire 03755, United States

9 [§]IPMA-Portuguese Institute of Sea and Atmosphere, Av. Brasilia, 1449-006, Lisbon,
10 Portugal

11 [¶]CIIMAR, Marine and Environmental Research Center, Rua dos Bragas, 289, 4050-123
12 Porto, Portugal

13

14

15 ***corresponding author:** address: Instituto de Investigacións Mariñas IIM-CSIC
16 Eduardo Cabello 6, 36208-Vigo, Spain
17 phone: +34 986231930
18 fax: +34 986292762
19 e-mail: calmecija@iim.csic.es
20

21 **ABSTRACT:**

22 Catalytic converters in automobiles have significantly increased the input of platinum
23 group elements (PGEs) to the environment and their coupled geochemical behavior has
24 been proposed. To check this hypothesis, Pt and Os concentrations and $^{187}\text{Os}/^{188}\text{Os}$
25 ratios were determined in sediment cores and interstitial waters from the Tagus Estuary
26 (SW Europe) affected by different traffic pressure.

27 Platinum concentration in surface sediments nearby the high traffic zone (up to $40 \text{ ng} \cdot \text{g}^{-1}$
28 ¹) indicated severe contamination. Although lower than Pt, Os enrichment was also
29 observed in surface sediments, with lower $^{187}\text{Os}/^{188}\text{Os}$ ratios than in deeper layers.
30 Dissolved Pt and Os in interstitial waters, $0.1\text{-}0.7 \text{ pg g}^{-1}$ and $0.03\text{-}0.10 \text{ pg g}^{-1}$
31 respectively, were higher than in typical uncontaminated waters. Results indicate two
32 sources of Pt and Os into the Tagus Estuary salt marshes: a regional input associated
33 with industrial activities, fossil fuel combustions and regional traffic; and a local source
34 linked to nearby traffic density emissions. Estimations of Os and Pt released by catalytic
35 converters support this two-source model. Differences in geochemical reactivity and
36 range of dispersion from their sources lead to a decoupled behavior of Os and Pt,
37 questioning the use of Os isotopes as proxies of PGE sources to the environment.

38

39 1. INTRODUCTION

40 Platinum group elements (PGE: ruthenium, rhodium, palladium, osmium, iridium and
41 platinum) are amongst the least abundant elements in the upper continental crust, where
42 their typical concentrations range from 20 pg g⁻¹ (Ir) to 500 pg g⁻¹ (Pt, Pd)¹. These
43 elements are relatively enriched in the Earth's mantle, and mantle-derived rocks host
44 some of the largest PGE deposits in the World (e.g. Bushveld Complex² and Noril'sk³).
45 The use of PGE in several human activities is increasing their environmental
46 concentrations^{4,5}; accordingly, it has been estimated that 86-98% of PGE total flux at
47 Earth's surface derives from anthropogenic activities⁶. One of the main application of
48 PGE (especially Pt, Pd and Rh) is their use in automobile catalytic converters in order to
49 reduce the emissions of CO, NO_x and SO₂⁷. This industrial application has been greatly
50 responsible for an exponential increase of the PGE demand over the past 40 years⁸. A
51 catalytic converter emits during its lifetime microparticles (1-63 μm⁹) covered by tiny
52 fragments (<0.3 μm down to the nanoparticle size¹⁰) of Pt, Pd, and Rh as active
53 components¹¹, and include smaller amounts of Os, Ir, and Ru as impurities¹². As a
54 result, elevated PGE concentrations are generally found in areas close to high traffic
55 density, especially within ~2 m near the road¹²⁻¹⁶. Evidence for a global scale PGE
56 contamination has also been observed in ice from Greenland and Antarctica^{17,18}.

57 Several studies have characterized the anthropogenic contribution of PGE in the
58 environment using the Os isotope signature (¹⁸⁷Os/¹⁸⁸O)¹⁹⁻²⁴ taking advantage of the
59 ¹⁸⁷Os/¹⁸⁸Os ratio as a tracer of a variety of anthropogenic and natural sources^{1,19,20,25,26}.
60 For example, the typical ¹⁸⁷Os/¹⁸⁸Os ratios of the PGE ores associated with mantle-
61 derived rocks, like the Bushveld complex², are 0.10 - 0.20²⁷ while ratios from the upper
62 continental crust are 1.05 ± 0.23¹, allowing the estimation of the Os anthropogenic

63 fraction in environmental samples^{23,25,25,26}. Assuming that Os and other PGE derive
64 from the same anthropogenic sources, the Os isotopic composition has been used to
65 estimate the anthropogenic fraction of Pt, Pd, and Rh, mainly in urban
66 environments^{19,21,22,24}. It has been suggested, however, that the anthropogenic Os
67 source(s) to the environment may be decoupled from the sources affecting other PGE
68 mainly due to the volatility of Os tetroxide²⁶. Therefore, the Pt, Pd, and Rh estimation
69 of anthropogenic contribution may be erroneously based on Os isotope signature²⁶. A
70 recent example of this decoupling is seen in the samples of PM₁₀ aerosols from Cape
71 Cod (USA)⁵ displaying Ir/Os ratios that are much greater than a natural ratio of ~1.

72 This study was designed to investigate the extent to which Pt is decoupled from Os in
73 natural environments, especially in such complex systems like salt marshes, a transition
74 environment between the continent and the ocean, where important physico-chemical
75 processes occur. Besides, salt marshes systems are particularly vulnerable to global
76 change and the sea level rise, and their characterization is taking an especial relevance.
77 We studied salt marsh sediments from the Tagus Estuary (SW Europe) that are subject
78 to different degrees of traffic influence¹³ and where the geochemistry of other trace
79 elements has been well-characterized²⁸⁻³⁰. The main aims of this research are: (1) to
80 better understand the geochemical behavior of Pt and Os in salt marshes; (2) quantify
81 the anthropogenic source of Pt and Os in sediments and interstitial waters from salt
82 marshes affected by different traffic impact; and (3) assess the coupling/decoupling
83 behavior of anthropogenic Pt and Os.

84 **2. MATERIAL AND METHODS**

85 ***2.1. Study area***

86 The Tagus Estuary, Portugal (SW Europe; Figure 1) is one of the largest estuaries in
87 Europe, with an extension of 320 km² and a volume of 1900 Hm³. The estuary is a
88 mesotidal system, where tidal water inundates large extensions of salt marshes on a
89 semidiurnal scale. Intertidal areas, including salt marshes, comprise around 40% of the
90 estuary. The Lisbon city is located at the northern margin but the whole estuary is
91 subjected high human pressure with around 3 million inhabitants living in this area,
92 several industries (chemicals, petrochemicals, fertilizers and pesticides) settled in the
93 margins³¹.

94 Cores were collected from two stations in the intertidal salt marshes at the southern
95 bank of Tagus Estuary, with different traffic pressure (Figure 1). High Traffic Station –
96 *Samouco* salt marsh– is located nearby a 17.2 km long motorway bridge that has been
97 operational since April 1998 with a daily average of 50,000 vehicles³². Past
98 anthropogenic activities in the area were negligible. Low Traffic Station –*Rosario* salt
99 marsh– is located nearby an important industrial area in the past, the Barreiro Chemical
100 Complex; this was one of the first heavy chemical plant industries in Portugal,
101 established around 1900 and its contaminating effects have been previously
102 reported^{33,34}. The highest industrial activity in this complex was between 1940's and
103 1970's. The world crises in the 1980's lead to the closure of some industries while other
104 were transformed for optimization purposes³⁴. In the last period a pyrite roasting plant
105 operated in the complex (1990³⁴), attempted to implement a method to extract Pt, Au
106 and Ag but the industrial processes were in an early stage of development and the low
107 yield make it a failure. Waste water treatments only started to be build up in the 1990's
108 and the most recent one, which covers this area (from Barreiro to Moita) did not start
109 until 2013. Thus in the last 2 decades no activity related with pyrite roasting operated in

110 the chemical complex of the Tagus estuary. Furthermore, the traffic pressure nearby the
111 Rosario salt marsh (Low Traffic Station) area is low.

112 **2.2. Sampling**

113 Several 20 cm long cores were sampled in the intertidal area of both salt marshes in
114 March 2011 (Low Traffic Station) and September 2011 (High Traffic Station).
115 Sediment cores were sectioned in situ every 2 cm in the first 10 cm and every 3 cm
116 between 10 and 20 cm depth. Each sample was stored in acid-clean high-density
117 polyethylene bottles avoiding the air presence inside to minimize sediment oxidation.
118 Bridge-gullypot sediment, representing automobile dust, including dust from catalytic
119 converters, was also sampled at the High Traffic Station (Figure 1). Interstitial waters
120 were extracted by centrifugation at 8000 rpm for 30 minutes at +4°C, filtered through
121 0.45 µm polycarbonate membranes, stored in acid-clean low-density polyethylene
122 bottles and acidified using Suprapur[®](Merck) HCl (pH≈1). A refractometer (Atago
123 S/Milla 0-100‰) was used to measure salinity in porewater. Sediment samples were
124 oven-dried (<60 °C) until constant weight and ground in an agate mortar. All materials
125 used were acid-cleaned and sample handling was done inside laminar flow hoods.
126 Procedural blanks were prepared using Milli-Q (Millipore) water.

127 **2.3. Analytical methods**

128 Platinum was determined in sediments and interstitial waters by means of catalytic
129 adsorptive cathodic stripping voltammetry (catalytic AdCSV)^{13,35,36}. For interstitial
130 waters, and in order to remove organic matter that may severely interfere during the
131 voltammetric determination of Pt, diluted (1:10) samples were UV-digested for 4 h as
132 described earlier³⁵ (see Figure S-1 for further details) in the presence of 22 mM H₂O₂

133 (TraceSelect[®] Ultra, Fluka). For interstitial waters, we obtained blanks of 0.003 ± 0.003
134 pg g^{-1} ($\bar{x} \pm SD$; $n=13$) and a detection limit ($x_{blank} + 3 \times SD_{blank}$) of 0.013 pg g^{-1}
135 (Table 1). For sediments, the removal of organic matter was achieved by ashing the
136 sediments (around 200 mg) at $800 \text{ }^\circ\text{C}$ in quartz crucibles¹³. Samples were then
137 transferred to 30 mL Teflon[®] vessels with screw caps (Savillex) for digestion with 5 mL
138 of concentrated HCl and 3 mL of concentrated HNO₃ (Merck Suprapur) at $195 \text{ }^\circ\text{C}$ (hot
139 plate temperature) for 4 h. Following digestion, the vessel caps were removed and the
140 acids evaporated at $195 \text{ }^\circ\text{C}$ to near dryness. The residue was re-dissolved with 1 mL of
141 concentrated HCl and 1 mL of concentrated H₂SO₄ (Fluka Trace Select), evaporated at
142 $195 \text{ }^\circ\text{C}$ until no fumes were observed and a near constant volume, comprising mostly
143 H₂SO₄, was attained. This procedure removes remnant HNO₃ which interferes with the
144 catalytic AdCSV Pt determination. Samples were cooled, diluted with 0.1 M HCl,
145 syringe-filtered ($0.45 \text{ }\mu\text{m}$) and made up to 25 mL in polypropylene volumetric flasks
146 (see Figure S-1 for further details). The detection limit ($x_{blank} + 3 \times SD_{blank}$) for a
147 typical mass of 200 mg of sediment was 37 pg g^{-1} (Table 1); the average blank value
148 was $24 \pm 4 \text{ pg g}^{-1}$ ($n=10$). The accuracy was checked using road dust certified reference
149 material (BCR-723³⁷) and good agreement was obtained with the certified
150 concentrations (Table 1).

151 Osmium concentration and isotopic composition in sediments and interstitial water were
152 determined using negative thermal ionization mass spectrometry (N-TIMS) using
153 previously established procedures at Dartmouth Radiogenic Isotope Geochemistry
154 Laboratory for water^{26,38,39} and for silicates^{40,41}. For interstitial waters the procedure is
155 described in brief as follows and outlined in the supporting information (Figure S-2).
156 About 30 to 50 g water was weighed in a quartz glass tube (“Carius tube”) and spiked

157 with ^{190}Os tracer solution. The sample was then frozen at $-20\text{ }^{\circ}\text{C}$ and placed in a High
158 Pressure Asher (HPA-S, Anton-Paar) immediately after adding $500\text{ }\mu\text{L}$ of *Jones*
159 *Reagent* ($\text{Cr}^{\text{IV}}\text{O}_3$ dissolved in $6\text{ M H}_2\text{SO}_4$), and heated to $300\text{ }^{\circ}\text{C}$ with a confining
160 pressures of 128 bar for 16 hours . This step allows Os in the sample to equilibrate with
161 tracer Os via conversion to a common oxidation state (OsO_4). Once the sample cooled it
162 was removed from HPA-S and OsO_4 (boiling point = $135\text{ }^{\circ}\text{C}$) separated by distillation
163 and trapped in ice-chilled HBr. This step reduces OsO_4 to hexabromoosmate, which is
164 further purified by microdistillation⁴². Blank for this procedure was found to be 0.0013
165 $\pm 0.0006\text{ pg g}^{-1}$ ($\bar{x} \pm SD$) with an $^{187}\text{Os}/^{188}\text{Os}$ ratio of 0.368 ± 0.044 ($n=2$) (Table 1).

166 For determination of Os concentration and isotope composition of sediments, we
167 followed the method described by Chen *et al.* 2006⁴⁰ and Wu *et al.* 2013⁴¹. Briefly, ~ 0.5
168 g of rock powder was spiked with ^{190}Os tracer solution in a Carius tube and attacked
169 with reverse *aqua-regia* (3 mL HCl plus 5 mL HNO_3) into the HPA-S ($300\text{ }^{\circ}\text{C}$, 128
170 bars, 16h). This procedure leaches out Os from the silicates and equilibrates it with
171 tracer Os by converting both a common oxidation state (OsO_4). Osmium tetraoxide is
172 then separated from bulk solution by solvent extraction with Br_2 (liquid) and purified
173 using microdistillation. Around 65% of the Os is recovered by this procedure⁴⁰. Blanks
174 were found to be $0.19 \pm 0.07\text{ pg g}^{-1}$ with $^{187}\text{Os}/^{188}\text{Os}$ ratio of 0.288 ± 0.003 ($n=2$).

175 The Os fraction of the sample in $0.5\text{ }\mu\text{L}$ of HBr was loaded on the pre-cleaned Pt side
176 filament using a fine polypropylene tubing fitted on a Hamilton microsyringe and dried
177 at 0.8 A . The typical load was centered and $1\text{--}2\text{ mm}$ of the filament length. Three drops
178 of fresh $\text{Ba}(\text{OH})_2$ emitter solution were loaded on top of the sample and dried. The
179 filament was then heated to 1.2 A for 6 s . Osmium isotopes were measured as OsO_3^- on
180 a Triton thermal ionization mass spectrometer (TIMS) using the double filament

181 geometry developed by Chen and Sharma (2009)³⁸. The data were corrected for oxygen
 182 isotope composition, mass fractionation and [Os] estimated by isotope dilution.
 183 Repeated (n=20) measurements of 1 pg laboratory standard (Max Planck Institute Os-1
 184 standard) gave an average $^{187}\text{Os}/^{188}\text{Os} = 0.1067 \pm 0.1\%$ (2σ RSD), which is within
 185 uncertainty of the established isotope value of 0.1069 for this standard. All reported
 186 $^{187}\text{Os}/^{188}\text{Os}$ ratios in this paper have a 2σ uncertainty of 2%. Table 1 provides some
 187 values of Os concentration and $^{187}\text{Os}/^{188}\text{Os}$ ratios for road dust reference materials³⁷ and
 188 compares our values with previous results⁴³ due to the absence of certified values.

189 Aluminum was determined by graphite furnace atomic absorption spectroscopy, after
 190 microwave digestion using a mixture of HCl, HNO₃ and HF⁴⁴. Blanks, detection limit
 191 and reference materials for Al analysis⁴⁵ are given in Table 1.

192 ***2.4. Estimation of enrichment factors and anthropogenic fractions of osmium and***
 193 ***platinum:***

194 Enrichment factors for Os (EF_{Os}) and Pt (EF_{Pt}) with respect to local background levels
 195 (Table 2) were calculated using the following equation:

$$196 \quad EF_{Pt \text{ or } Os} = \frac{([Pt \text{ or } Os]/[Al])_{sample}}{([Pt \text{ or } Os]/[Al])_{local \ background}} \quad (1)$$

197 The anthropogenic fraction of Pt (AF_{Pt} , %) was calculated normalizing by Pt/Al instead
 198 of using Pt/Os ratios²⁵ to avoid the influence of coupled/decoupled behavior of Os and
 199 Pt by means of:

$$200 \quad AF_{Pt}(\%) = \left(1 - \frac{([Pt]/[Al])_{local \ background}}{([Pt]/[Al])_{sample}}\right) \times 100 = \left(1 - \frac{1}{EF_{Pt}}\right) \times 100 \quad (2)$$

201 The equation proposed by Rauch^{23,25} was used to calculate the anthropogenic fraction of
202 Os (AF_{Os} , %), based on the isotopic compositions, but using local background levels
203 instead of the average $^{187}\text{Os}/^{188}\text{Os}$ of the eroded upper continental crust¹ (Table 2).

$$204 \quad AF_{Os} (\%) = \frac{\left(\frac{^{187}\text{Os}}{^{188}\text{Os}}\right)_{local\ background} - \left(\frac{^{187}\text{Os}}{^{188}\text{Os}}\right)_{sample}}{\left(\frac{^{187}\text{Os}}{^{188}\text{Os}}\right)_{local\ background} - \left(\frac{^{187}\text{Os}}{^{188}\text{Os}}\right)_{anthropogenic}} \times 100 \quad (3)$$

205 Natural and anthropogenic concentrations of Os and Pt were calculated applying this AF
206 (%) to the total concentrations²⁵.

207 **3. RESULTS**

208 **3.1. Sedimentary background**

209 Sediments from both stations are composed by fine grained sedimentary material. The
210 Al_2O_3 content ranged from 9 to 23%, with values increasing with depth at both sites
211 (Table 2). Organic matter content ($\text{LOI}_{550\text{ }^\circ\text{C}}$, %) in sediments was $6.8 \pm 3.3\%$ and $6.6 \pm$
212 2.7% at Low and High Traffic Station (except for the upper 4 cm at High Traffic
213 Station where values up to 23% were found, Figure S-3). The oxygen penetration depth
214 was very low at both sites (Figure S-3). At High Traffic Station, oxygen saturation was
215 below the detection limit even in the uppermost layers; at Low Traffic Station, oxygen
216 was present in the upper 20 cm ($3.1 \pm 4.5\%$), and below detection limit at higher
217 depths. No macrofauna were found in the collected sediments. This sediment
218 characteristics are in line with results obtained by Caetano et al. (2008; 2012)^{28,29} in
219 several marshes from the Tagus estuary. Other parameters analyzed in interstitial waters
220 (Eh, salinity, dissolved Fe, Mn and total reduced sulfur species) are showed in the
221 supporting information (Figure S-3).

222 **3.2. Concentrations of Pt and Os in sediment**

223 Platinum concentrations in sediments cores from both stations showed a surface peak;
224 the concentration at the High Traffic Station (40100 pg g^{-1}) is about 15 times higher
225 than that at the Low Traffic Station (2750 pg g^{-1} ; Figure 2, Table 2; for the complete
226 dataset see Table S-1). Platinum concentration decreases with depth, reaching similar
227 average background values below 5 cm (Figure 2, Table 2): 670 ± 89 (High Traffic
228 Station; $\bar{x} \pm SD$, $n=5$) and $682 \pm 240 \text{ pg g}^{-1}$ (Low Traffic Station; $n=4$). Osmium
229 concentrations ranged from 25 to 68 pg g^{-1} , but no trend with depth was observed
230 (Figure 2, Table 2): surface Os concentrations were 47 and 51 pg g^{-1} for the High
231 Traffic Station and Low Traffic Station, respectively, whereas the average
232 concentrations for the deeper layers ($>5\text{cm}$ depth) were $36 \pm 6.8 \text{ pg g}^{-1}$ (High Traffic
233 Station) and $62 \pm 6.7 \text{ pg g}^{-1}$ (Low Traffic Station). The sample from the motorway
234 bridge gullypot at High Traffic Station, which is representative of the road runoff
235 source⁴⁶, contained 157000 pg g^{-1} of Pt and 114 pg g^{-1} of Os (Table 2).

236 **3.3. Concentrations of Pt and Os in overlying and interstitial waters**

237 To the knowledge of the authors, the data of dissolved Pt and Os for interstitial waters
238 obtained in this study (Figure 2; Table S-1) are the first reported in the literature. The
239 values obtained for Pt ranged from 0.14 to 0.66 pg g^{-1} (with the exception of a 2.5 pg g^{-1}
240 peak at Low Traffic Station) and between 0.028 and 0.11 pg g^{-1} for Os. The average
241 dissolved concentrations of Pt ($0.21 \pm 0.07 \text{ pg g}^{-1}$) and Os ($0.037 \pm 0.011 \text{ pg g}^{-1}$) at the
242 Low Traffic Station were, in general, lower than at High Traffic Station ($0.55 \pm 0.07 \text{ pg}$
243 g^{-1} for Pt and $0.074 \pm 0.027 \text{ pg g}^{-1}$ for Os). In the overlying water, Pt and Os
244 concentrations were 0.164 pg g^{-1} and 0.019 pg g^{-1} , respectively, being lower than those
245 found in interstitial waters for Os.

246 3.4. $^{187}\text{Os}/^{188}\text{Os}$ ratios in sediments and interstitial waters

247 The $^{187}\text{Os}/^{188}\text{Os}$ ratios in the sediments ranged from 0.91 to 1.18, while in interstitial
248 waters values varied between 0.85 and 1.07 and in the overlying water the ratio was
249 0.92 (Figure 2, Table 2, complete dataset in Table S-1). Gullypot sediment exhibits the
250 highest $^{187}\text{Os}/^{188}\text{Os}$ ratio, 1.26. Profiles of $^{187}\text{Os}/^{188}\text{Os}$ ratios in interstitial waters and
251 sediments had a similar trend at High Traffic Station, i.e., decreasing towards the
252 surface. Ratios in sediments and interstitial waters from Low Traffic Station were
253 similar in the upper 8 cm, but values in sediments increased markedly towards the
254 bottom at a higher extent than in interstitial waters.

255 DISCUSSION

256 4.1 The anthropogenic impact on Pt and Os

257 Previous studies have reported typical Pt and Os concentrations for continental crust
258 ($\text{Pt} = 510 \text{ pg g}^{-1}$, $\text{Os} = 31 \text{ pg g}^{-1}$) and contaminated sediments ($\text{Pt} = 10^3\text{-}10^5 \text{ pg g}^{-1}$, $\text{Os} =$
259 $4 \times 10^1\text{-}8 \times 10^2 \text{ pg g}^{-1}$, more information in Table S-2^{12,15,16,19,20,22,23,46-53}). Platinum found
260 in the upper layers (<4 cm) from the two salt marshes, as well as in the gullypot, were
261 elevated in comparison to background values (Table 2). The enrichment factor for Pt
262 (EF_{Pt} , equation 1) was 119 in the upper sediments (<2 cm) of High Traffic Station, but
263 decreased sharply to 8 at 2 - 4 cm depth. In the Low Traffic Station, the enrichment was
264 much lower and restricted to the surface layer (<2cm, $EF_{\text{Pt}} = 4$); for deeper layers, the
265 calculated enrichment were within the typical natural variability of background
266 sediments (Table 2). Noteworthy, the EF_{Os} in sediments from both High and Low
267 Traffic Stations suggest minor to null anthropogenic input. At Low Traffic Station a
268 EF_{Os} close to 1 (i.e. no enrichment) was obtained despite the higher Os concentrations

269 compared to High Traffic Station. The calculated anthropogenic fractions (*AF*;
270 equations 2-3) in the upper layer of High Traffic Station showed that 99 % of Pt (39700
271 pg g^{-1}) was from anthropogenic origin but only 15 % of Os (7 pg g^{-1}). In the Low
272 Traffic Station the anthropogenic contribution was 77 % for Pt (2120 pg g^{-1}) and 18 %
273 for Os (9 pg g^{-1}) in the surface sediments. Significantly, both stations have similar Os
274 contribution from anthropogenic sources, but a 20-fold difference for Pt.

275 The deposition rates of anthropogenic Pt were calculated for the layers where the
276 anthropogenic fraction (AF_{Pt} , Table 2) was found to be greater than 50% (using the
277 sedimentation rates reported earlier⁵⁴ for both stations, see Figure S-4 for a detailed
278 explanation of the calculations); these are the upper 4 and 2 cm at the High and Low
279 Traffic Station, respectively. The average estimated deposition rates are $6,600 \text{ ng Pt m}^{-2}$
280 y^{-1} at the Low Traffic Station (0 - 2 cm) and comparable to a deposition rate of a) $8,400$
281 $\text{ng Pt m}^{-2} \text{ y}^{-1}$ in urban environments of Germany⁵⁵, and b) $9,000 \pm 5,000 \text{ ng Pt m}^{-2} \text{ y}^{-1}$ for
282 the period 1992-2002 in an urban lake in USA²². In contrast, the Pt deposition rates at
283 the High Traffic Station are $310,000 \text{ ng Pt m}^{-2} \text{ y}^{-1}$ (0 - 2 cm) and $17,000 \text{ ng Pt m}^{-2} \text{ y}^{-1}$ (2
284 - 4 cm) indicating a substantially larger anthropogenic input of Pt at this site.

285 Since the automobile traffic over the motorway bridge is the most relevant activity at
286 the High Traffic Station, we evaluated whether this source alone may explains the Pt
287 input. The estimation of the Pt input from catalytic converters was made based on the
288 following information: (i) 50,000 vehicles per day passing through the bridge³²; (ii) an
289 estimation of 37 % of vehicles with gasoline engine and 63 % with diesel⁵⁶; (iii) a
290 release of 400 - 800 ng Pt Km^{-1} and 108 - 150 ng Pt Km^{-1} for new (less than 1 year) and
291 old (more than 1 year) diesel vehicles, respectively, from laboratory measurements¹¹ ;
292 (iv) a release of 100 ng Pt Km^{-1} and 6-8 ng Pt Km^{-1} for new and old gasoline vehicles,

293 respectively, from laboratory measurements¹¹; (v) a release of 270 ng Pt Km⁻¹ for every
294 car, as an alternative based on environmental estimations^{51,55}; (vi) the bridge is 17.2 Km
295 long; (vii) 4928 days have passed since the bridge started to operate (April 1998) until
296 the sampling (September 2011). Based on these, the bridge car traffic has resulted in a
297 release of 450 or 1140 g of Pt to the environment (following laboratory measurements¹¹
298 or environmental estimations^{51,55}; see Figure S-5 and Table S-3 for further information
299 on this estimation).

300 Given that (i) almost all the Pt contamination is in the top 4-cm sediment layer based on
301 the AF_{Pt} obtained for the top 4 cm (Table 2), and (ii) a sediment deposition of 3.9 cm
302 since the bridge was open in 1998 (Figure S-4) is derived using the sedimentation rates
303 reported previously⁵⁴, the estimated Pt enrichment in the vicinity of the motorway
304 bridge may be calculated taking into account the dispersion range of the emitted
305 particles from catalytic converters. If a 2-m dispersion is taken into consideration based
306 on studies in roadside soil^{12,49,52}, an enrichment of 61,000-160,000 pg g⁻¹ of Pt would be
307 expected in the vicinity of the road bridge (depending on the model of emissions^{11,51,55}).
308 However, this estimated range of enrichment is higher than the concentration found in
309 the sediments from the High Traffic Station (40,000 pg g⁻¹). The difference may be due
310 to higher dispersion of particles from the bridge than from a regular road. Accordingly,
311 and using the estimations above, a particle dispersion of 16 m would be needed to
312 explain the enrichment found at High Traffic Station (or 6 m following laboratory
313 measurements¹¹; more information in Figure S-5 and Table S-3).

314 The release of Os from traffic at High Traffic Station was estimated following the
315 previous assumptions (number of vehicles, length of bridge, etc) and with (i) the release
316 of almost all the Os from catalytic converters is during the first year of vehicle life

317 (approximately first 20,000 Km) due to its volatile character⁵⁷; and (ii) catalytic
318 converters contain 6 - 228 pg g⁻¹ of Os⁵⁷. On this basis, an estimation of 1.7 mg input of
319 Os to the roadside was found (further information Figure S-5 and Table S-3). This value
320 could explain an input of 0.24 pg g⁻¹ (2 m dispersion) or 0.03 pg g⁻¹ (15 m, using the
321 dispersion calculated for Pt) in the first 4 cm of the sediment, and a deposition of 1.8 ng
322 m⁻² y⁻¹ or 0.24 ng m⁻² y⁻¹ (depending on 2 or 15 m of dispersion). On the top of that,
323 considering that Os is released as the gaseous OsO₄ species, it is expected that the
324 dispersion is well higher than that considered for Pt –which is released as particles– and
325 therefore the Os inputs here indicated are an upper limit estimation, minimizing its local
326 deposition even further. These calculations show that the Os supply from nearby traffic
327 is significantly lower than the typical regional atmospheric deposition; accordingly,
328 Rauch *et al.* 2010²⁰ estimated an atmospheric deposition during the last 40 years around
329 30 ng m⁻² y⁻¹ of Os from a peat bog located in the NW Iberian Peninsula. Assuming this
330 deposition rate in High Traffic Station sediments, an increase of 3.9 pg g⁻¹ of Os would
331 be expected in the top 4-cm sediment layer, i.e., which is 16 - 160 times higher than the
332 Os that nearby traffic may supply.

333 The surface sediments have low ¹⁸⁷Os/¹⁸⁸Os ratios compared to the background. The
334 presence of a less radiogenic source in the surface is consistent with the surface
335 anthropogenic Os contribution at both stations (Table 2). The ¹⁸⁷Os/¹⁸⁸Os ratios against
336 the inverse of Os concentrations are plotted in Figure 3. Four potential sources – fossil
337 fuels (radiogenic, Os = 210 pg g⁻¹, ¹⁸⁷Os/¹⁸⁸Os = 3.7)^{58,59}; Iberian pyrite belt (radiogenic,
338 Os = 330 pg g⁻¹, ¹⁸⁷Os/¹⁸⁸Os = 9.7)⁵³; PGE ores (unradiogenic, Os = 3 10⁵ pg g⁻¹,
339 ¹⁸⁷Os/¹⁸⁸Os = 0.2)^{20,60,61} and eroded continental crust (Os = 31 pg g⁻¹, ¹⁸⁷Os/¹⁸⁸Os =
340 1.05)¹– have been identified (triangles, Figure 3) to help explain the Os isotope

341 compositions in the sediment core samples. Sediments from High Traffic Station
342 (diamonds, Figure 3) fall close to the eroded continental crust endmember, but PGE
343 ores appear to influence surface samples. Interestingly, the interpretation of $^{187}\text{Os}/^{188}\text{Os}$
344 ratios in sediments from Low Traffic Station (dots, Figure 3) is more complex. Surface
345 sediments show an isotopic composition similar to High Traffic Station, pointing a link
346 to the PGE ores source. However, deeper sediments show a higher influence of a more
347 radiogenic source(s) like fossil fuels and the Iberian Pyrite Belt. The higher industrial
348 activity of Barreiro Chemical Complex due to a pyrite roasting (that processed pyrite
349 from Iberian Pyritic Belt) and a smelter from a steel factory, all of them using fossil
350 combustibles to perform their activity, may explain the fossil fuels and the pyrite belt
351 contribution. Moreover, the gullypot sediment sample also shows an important
352 contribution of this more radiogenic source(s), being within the mixing line of fossil
353 fuels and PGE ores; thus, anthropogenic sources (fossil fuels, pyrite belt and PGE ores)
354 influence the deeper sediment isotopic values at Low Traffic Station. Rauch *et al.*
355 2010²⁰ defined similar sources to explain the isotopic composition of a peat bog in the
356 NW Iberian Península where their effect was detected for the last 50 years, including
357 the Iberian Pyritic Belt mining activities, although geographically their study area was
358 farther from the mining area than our study area.

359 Concentrations of Pt and Os in interstitial waters (Pt: 0.14 - 0.66 pg g^{-1} , Os: 0.028 - 0.11
360 pg g^{-1}) were higher than typical values for oceanic waters (0.04 - 0.3 and 0.008 pg g^{-1}
361 for Pt and Os, respectively⁶²), and for estuarine waters (S=30 ‰; 0.08 - 0.11 pg g^{-1} for
362 Pt³⁵ and 0.01 pg g^{-1} for Os⁶³). Using North Atlantic waters^{35,38} as a reference for
363 interstitial waters the Os enrichment was higher than Pt enrichment, suggesting a lower
364 mobility of Pt compared to Os, which appears to be easily mobilized in the interstitial

365 water. Accordingly, the similar Os isotopic composition in interstitial waters and
366 sediments suggest the existence of quasi-equilibrium conditions between both phases,
367 indicating fast reaction kinetics for this element in contrast with the well-known
368 chemical inertness of Pt in surface environments. The dissolved Os profiles in
369 interstitial waters, with concentrations increasing with depth, support the idea of
370 diffusive fluxes from the sediments to the overlying water. Interestingly, the isotopic
371 composition of overlying water shows almost the same ratios than open oceanic waters
372 (0.95^{64} for the North Atlantic) suggesting that salt marshes may act as a source of Os to
373 the ocean. Nevertheless, the export of Os would deplete the pool in sediments if not
374 balanced by equivalent inputs, therefore requiring an import to the sediment by
375 atmospheric deposition. Also, the sediment-water partition of Os – and eventually the
376 diffusive fluxes – appears to be affected by the amount of organic matter and/or
377 sulfides, as indicated by the increase in the sediment/water partition coefficients with
378 these two variables (see Figure S-6, supporting information).

379 ***4.2 Os-Pt decoupling in the environment***

380 The Pt/Os ratios of sediments show a wide range of values (Figure 2, Table 2). Ratios of
381 Pt/Os for background sediments at High (19 ± 5) and Low Traffic Stations (11 ± 5)
382 were comparable to average eroded continental crust (16.5^1 , Figure 2). However, ratios
383 in surface sediments near the bridge (High Traffic Station) were ~45 times higher than
384 background levels and 5 times the background at the Low Traffic Station. The highest
385 Pt/Os ratio was found in the gullypot sediment, which was twice the value in surface
386 sediments at High Traffic Station. In addition, if Pt and Os were derived only from
387 anthropogenic sources, ratios (calculated using the amount of Pt and Os and applying
388 them the AF_{Pt} and AF_{Os}) would be 5600 and 220 in High and Low Traffic Station,

389 respectively. Thus, the regional common source indentified in the Low Traffic Station
390 (Pt sedimentation rate $6,600 \text{ ng m}^{-2} \text{ y}^{-1}$), has a Pt/Or ratio of 220. The other local source
391 (Pt sedimentation rate $300,000 \text{ ng m}^{-2} \text{ y}^{-1}$) that is related to vehicular traffic emissions
392 (High Traffic Station) had Pt/Os ratio ~ 5600 , which is in agreement with the elevated
393 ratios for the particles emitted from catalytic converters (4×10^6 - 2×10^8 ^{11,12,57}).

394 In interstitial waters Pt/Os ratios are lower and within a narrow range of 5 - 12 in all the
395 profiles (Figure 2), which are close to ratios for North Atlantic waters (Pt/Os = 5, Figure
396 2, light blue straight line; Table 2), except for ratio for the Pt peak at Low Traffic
397 Station (Pt/Os = 57; 14.5 cm). The absence of a surface peak in Pt/Os agrees with the
398 lower reactivity of Pt respect to Os. The results obtained suggest different post-
399 depositional processes for anthropogenic Pt and Os: while most of Pt remains within the
400 sediment (mainly as particles), Os appears to reach equilibrium between the sediment
401 and the interstitial waters and eventually exported to the estuary.

402 Our results point to the existence of two different anthropogenic sources of Pt and Os to
403 the salt marshes at Tagus Estuary:

404 -a regional source, with Pt/Os ~ 220 linked to human activities around Lisbon
405 area including large scale traffic^{22,55} and industrial effects with emphasis to fossil fuels
406 as a relevant source.

407 -a local source, linked to nearby traffic emissions and affected by the degree of
408 dispersion (e.g. bridge>regular road).

409 These results support the hypothesis of a decoupled behavior between Pt and Os in the
410 environment relative to both sources and mechanisms of release and dispersion, as well
411 as their different reactivity and mobility. Accordingly, Pt is dispersed as solid and non-

412 reactive particulates, whereas Os is emitted as gaseous OsO₄ and when settled displays
413 a higher mobility. This should be taken into consideration when using the Os isotope
414 ratios for the reconstruction of the sources and contamination of platinum group
415 elements in environmental matrices.

416 **ACKNOWLEDGMENTS:**

417 The CSIC, under the program JAE-PreDoc (*Junta para la Ampliación de Estudios*) co-
418 funded by the *Fondo Social Europeo* (FSE), is greatly acknowledge for the predoctoral
419 and post-doctoral fellowships to C. Almécija and J. Santos-Echeandía, respectively, as
420 well as for the funding for a stay at Dartmouth College (C. Almécija). We also thank the
421 *Universidade de Vigo* and *Facultade de Ciencias do Mar* for the PhD program in
422 Oceanography and Susana Calvo (IIM-CSIC) and Joana Raimundo (IPMA) for
423 technical work.

424

425 **Supporting information available:** Schemes for detailed processes of Pt and Os
426 analysis in interstitial waters and sediments; supplementary methods of analysis for
427 auxiliary parameters (Eh, O₂, salinity, loss on ignition, dissolved Fe, Mn and total
428 reduced sulfur species); correlation between the partition coefficient of Os in sediments
429 and interstitial waters vs. loss on ignition and sulfur species; a further explanation for
430 the sedimentation rates and deposited thickness calculated for each station and
431 calculations for the Pt and Os release by catalytic converters. The complete dataset is
432 also included, as well as some values of Pt and Os in natural con contaminated
433 sediments. This information is available free of charge via the Internet at
434 <http://pubs.acs.org>.

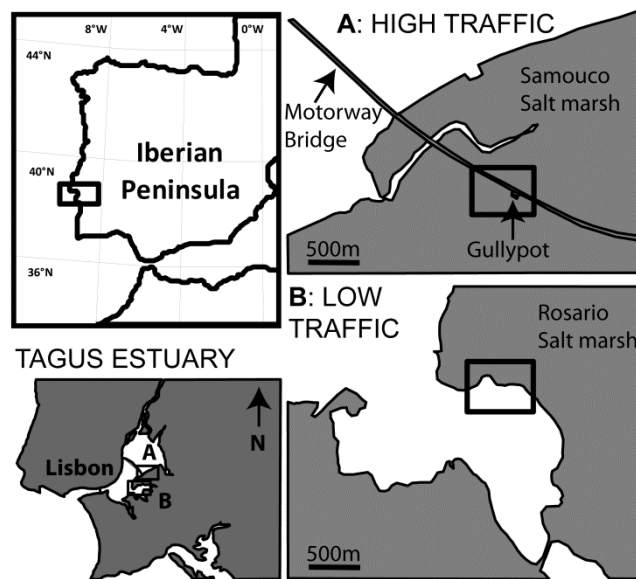
435

- 437 (1) Peucker-Ehrenbrink, B.; Jahn, B. Rhenium-osmium isotope systematics and
438 platinum group element concentrations: Loess and the upper continental crust.
439 *Geochem. Geophys. Geosystems* **2001**, *2*, 1061.
- 440 (2) Naldrett, T.; Kinnaird, J.; Wilson, A.; Chunnett, G. Concentration of PGE in the
441 Earth's Crust with Special Reference to the Bushveld Complex. *Earth Sci. Front.*
442 **2008**, *15* (5), 264–297.
- 443 (3) Malitch, K. N.; Latypov, R. M. Re-Os and S isotope constraints on timing and
444 source heterogeneity of PGE-Cu-Ni sulfide ores: A case study at the Talnakh
445 ORE junction, Noril'sk Province, Russia. *Can. Mineral.* **2011**, *49* (6), 1653–
446 1677.
- 447 (4) Rauch, S.; Morrison, G. M. Environmental relevance of the platinum-group
448 elements. *Elements* **2008**, *4* (4), 259–263.
- 449 (5) Sen, I. S.; Peucker-Ehrenbrink, B.; Geboy, N. Complex Anthropogenic Sources
450 of Platinum Group Elements in Aerosols on Cape Cod, USA. *Environ. Sci.*
451 *Technol.* **2013**, *47* (18), 10188–10196.
- 452 (6) Sen, I. S.; Peucker-Ehrenbrink, B. Anthropogenic Disturbance of Element Cycles
453 at the Earth's Surface. *Environ. Sci. Technol.* **2012**, *46* (16), 8601–8609.
- 454 (7) Farrauto, R. J.; Heck, R. M. Catalytic converters: state of the art and perspectives.
455 *Catal. Today* **1999**, *51* (3), 351–360.
- 456 (8) Johnson Matthey. Market Data Tables. www.platinum.matthey.com
- 457 (9) Artelt, S.; Kock, H.; König, H. P.; Levsen, K.; Rosner, G. Engine dynamometer
458 experiments: platinum emissions from differently aged three-way catalytic
459 converters. *Atmos. Environ.* **1999**, *33* (21), 3559–3567.
- 460 (10) Prichard, H. M.; Fisher, P. C. Identification of platinum and palladium particles
461 emitted from vehicles and dispersed into the surface environment. *Environ. Sci.*
462 *Technol.* **2012**, *46* (6), 3149–3154.
- 463 (11) Palacios, M. A.; Gomez, M. M.; Moldovan, M.; Morrison, G.; Rauch, S.;
464 McLeod, C.; Ma, R.; Laserna, J.; Lucena, P.; Caroli, S. Platinum-group elements:
465 quantification in collected exhaust fumes and studies of catalyst surfaces. *Sci.*
466 *Total Environ.* **2000**, *257* (1), 1–15.
- 467 (12) Fritsche, J.; Meisel, T. Determination of anthropogenic input of Ru, Rh, Pd, Re,
468 Os, Ir and Pt in soils along Austrian motorways by isotope dilution ICP-MS. *Sci.*
469 *Total Environ.* **2004**, *325* (1), 145–154.
- 470 (13) Cobelo-García, A.; Neira, P.; Mil-Homens, M.; Caetano, M. Evaluation of the
471 contamination of platinum in estuarine and coastal sediments (Tagus Estuary and
472 Prodelta, Portugal). *Mar. Pollut. Bull.* **2011**, *62* (3), 646–650.
- 473 (14) Tuit, C. B.; Ravizza, G. E.; Bothner, M. H. Anthropogenic platinum and
474 palladium in the sediments of Boston Harbor. *Environ. Sci. Technol.* **2000**, *34* (6),
475 927–932.
- 476 (15) Whiteley, J. D.; Murray, F. Autocatalyst-derived platinum, palladium and
477 rhodium (PGE) in infiltration basin and wetland sediments receiving urban
478 runoff. *Sci. Total Environ.* **2005**, *341* (1), 199–209.
- 479 (16) Sutherland, R. A.; Pearson, D. G.; Ottley, C. J. Platinum-group elements (Ir, Pd,
480 Pt and Rh) in road-deposited sediments in two urban watersheds, Hawaii. *Appl.*
481 *Geochem.* **2007**, *22* (7), 1485–1501.
- 482 (17) Barbante, C.; Veyseyre, A.; Ferrari, C.; Van De Velde, K.; Morel, C.;
483 Capodaglio, G.; Cescon, P.; Scarponi, G.; Boutron, C. Greenland snow evidence

- 484 of large scale atmospheric contamination for platinum, palladium, and rhodium.
485 *Environ. Sci. Technol.* **2001**, 35 (5), 835–839.
- 486 (18) Soyol-Erdene, T.-O.; Huh, Y.; Hong, S.; Hur, S. D. A 50-year record of platinum,
487 iridium, and rhodium in Antarctic snow: volcanic and anthropogenic sources.
488 *Environ. Sci. Technol.* **2011**, 45 (14), 5929–5935.
- 489 (19) Esser, B. K.; Turekian, K. K. Anthropogenic osmium in coastal deposits.
490 *Environ. Sci. Technol.* **1993**, 27 (13), 2719–2724.
- 491 (20) Rauch, S.; Peucker-Ehrenbrink, B.; Kylander, M. E.; Weiss, D. J.; Martinez-
492 Cortizas, A.; Heslop, D.; Olid, C.; Mighall, T. M.; Hemond, H. F. Anthropogenic
493 forcings on the surficial osmium cycle. *Environ. Sci. Technol.* **2010**, 44 (3), 881–
494 887.
- 495 (21) Rauch, S.; Hemond, H. F.; Peucker-Ehrenbrink, B.; Ek, K. H.; Morrison, G. M.
496 Platinum group element concentrations and osmium isotopic composition in
497 urban airborne particles from Boston, Massachusetts. *Environ. Sci. Technol.*
498 **2005**, 39 (24), 9464–9470.
- 499 (22) Rauch, S.; Hemond, H. F.; Peucker-Ehrenbrink, B. Recent changes in platinum
500 group element concentrations and osmium isotopic composition in sediments
501 from an urban lake. *Environ. Sci. Technol.* **2004**, 38 (2), 396–402.
- 502 (23) Rauch, S.; Hemond, H. F.; Peucker-Ehrenbrink, B. Source characterisation of
503 atmospheric platinum group element deposition into an ombrotrophic peat bog. *J.*
504 *Environ. Monit.* **2004**, 6 (4), 335–343.
- 505 (24) Ravizza, G. E.; Bothner, M. H. Osmium isotopes and silver as tracers of
506 anthropogenic metals in sediments from Massachusetts and Cape Cod bays.
507 *Geochim. Cosmochim. Acta* **1996**, 60 (15), 2753–2763.
- 508 (25) Rauch, S.; Peucker-Ehrenbrink, B.; Hemond, H. F. Source characterization of
509 platinum group elements using the isotopic composition of osmium. In *Palladium*
510 *Emissions in the Environment*; Zereini, F, Alt, F, Eds.; Springer, 2006; pp 640.
- 511 (26) Sharma, M. Applications of osmium and iridium as biogeochemical tracers in the
512 environment. In *Handbook of Environmental Isotope Geochemistry*; Baskaran,
513 M. Ed.; Springer, 2011; pp. 951.
- 514 (27) Schoenberg, R.; Kruger, F. J.; Nägler, T. F.; Meisel, T.; Kramers, J. D. PGE
515 enrichment in chromitite layers and the Merensky Reef of the western Bushveld
516 Complex; a Re-Os and Rb-Sr isotope study. *Earth Planet. Sci. Lett.* **1999**, 172 (1-
517 2), 49–64.
- 518 (28) Caetano, M.; Bernárdez, P.; Santos-Echeandia, J.; Prego, R.; Vale, C. Tidally
519 driven N, P, Fe and Mn exchanges in salt marsh sediments of Tagus estuary (SW
520 Europe). *Environ. Monit. Assess.* **2012**, 184 (11), 6541–6552.
- 521 (29) Caetano, M.; Vale, C.; Cesário, R.; Fonseca, N. Evidence for preferential depths
522 of metal retention in roots of salt marsh plants. *Sci. Total Environ.* **2008**, 390 (2),
523 466–474.
- 524 (30) Santos-Echeandía, J.; Vale, C.; Caetano, M.; Pereira, P.; Prego, R. Effect of tidal
525 flooding on metal distribution in pore waters of marsh sediments and its transport
526 to water column (Tagus estuary, Portugal). *Mar. Environ. Res.* **2010**, 70 (5), 358–
527 367.
- 528 (31) Valentim, J. M.; Vaz, N.; Silva, H.; Duarte, B.; Caçador, I.; Dias, J. M. Tagus
529 estuary and Ria de Aveiro salt marsh dynamics and the impact of sea level rise.
530 *Estuar. Coast. Shelf Sci.* **2013**, 130, 138–151.
- 531 (32) Instituto de Infraestruturas Rodoviárias IP (Portugal). *Relatório de Tráfego na*
532 *rede nacional de auto-estradas 3º Trimestre de 2013*; 2013. www.inir.pt

- 533 (33) Caetano, M.; Fonseca, N.; Cesário Carlos Vale, R. Mobility of Pb in salt marshes
534 recorded by total content and stable isotopic signature. *Sci. Total Environ.* **2007**,
535 *380* (1), 84–92.
- 536 (34) Mil-Homens, M.; Caetano, M.; Costa, A. M.; Lebreiro, S.; Richter, T.; de Stigter,
537 H.; Trancoso, M. A.; Brito, P. Temporal evolution of lead isotope ratios in
538 sediments of the Central Portuguese Margin: A fingerprint of human activities.
539 *Mar. Pollut. Bull.* **2013**, *74* (1), 274–284.
- 540 (35) Cobelo-García, A.; López-Sánchez, D. E.; Almécija, C.; Santos-Echeandia, J.
541 Behaviour of Platinum During Estuarine Mixing (Pontevedra Ria, NW Iberian
542 Peninsula). *Mar. Chem.* **2013**, *150*, 11–18.
- 543 (36) Van den Berg, C. M. G.; Jacinto, G. S. The determination of platinum in sea
544 water by adsorptive cathodic stripping voltammetry. *Anal. Chim. Acta* **1988**, *211*,
545 129–139.
- 546 (37) Institute of Reference Materials and Measurements. Certified Reference Material
547 2013. irmm.jrc.ec.europa.eu/
- 548 (38) Chen, C.; Sharma, M. High precision and high sensitivity measurements of
549 osmium in seawater. *Anal. Chem.* **2009**, *81* (13), 5400–5406.
- 550 (39) Sharma, M.; Chen, C.; Blazina, T. Osmium contamination of seawater samples
551 stored in polyethylene bottles. *Limnol. Oceanogr. Methods* **2012**, *10*, 618–630.
- 552 (40) Chen, C.; Sharma, M.; Bostick, B. C. Lithologic controls on osmium isotopes in
553 the Rio Orinoco. *Earth Planet. Sci. Lett.* **2006**, *252* (1–2), 138–151.
- 554 (41) Wu, Y.; Sharma, M.; LeCompte, M. A.; Demitroff, M. N.; Landis, J. D. Origin
555 and provenance of spherules and magnetic grains at the Younger Dryas boundary.
556 *Proc. Natl. Acad. Sci.* **2013**, *110* (38), E3557–E3566.
- 557 (42) Birck, J. L.; Barman, M. R.; Capmas, F. Re-Os Isotopic Measurements at the
558 Femtomole Level in Natural Samples. *Geostand. Newsl.* **1997**, *21* (1), 19–27.
- 559 (43) Meisel, T.; Fellner, N.; Moser, J. A simple procedure for the determination of
560 platinum group elements and rhenium (Ru, Rh, Pd, Re, Os, Ir and Pt) using ID-
561 ICP-MS with an inexpensive on-line matrix separation in geological and
562 environmental materials. *J. Anal. At. Spectrom.* **2003**, *18* (7), 720–726.
- 563 (44) Lambie, K. J.; Hill, S. J. Microwave digestion procedures for environmental
564 matrices. Critical Review. *Analyst* **1998**, *123* (7), 103R – 133R.
- 565 (45) National Researcher council Canada. Marine sediment reference materials for
566 trace metals and other constituents. www.nrc-cnrc.gc.ca/index.html
- 567 (46) Wei, C.; Morrison, G. M. Platinum analysis and speciation in urban gullypots.
568 *Anal. Chim. Acta* **1994**, *284* (3), 587–592.
- 569 (47) Colodner, D. C.; Boyle, E. A.; Edmond, J. M.; Thomson, J. Post-depositional
570 mobility of platinum, iridium and rhenium in marine sediments. *Nature* **1992**,
571 *358*, 402–404.
- 572 (48) Fliegel, D.; Berner, Z.; Eckhardt, D.; Stüben, D. New data on the mobility of Pt
573 emitted from catalytic converters. *Anal. Bioanal. Chem.* **2004**, *379* (1), 131–136.
- 574 (49) Schäfer, J.; Puchelt, H. Platinum-Group-Metals (PGM) emitted from automobile
575 catalytic converters and their distribution in roadside soils. *J. Geochem. Explor.*
576 **1998**, *64* (1), 307–314.
- 577 (50) Prichard, H. M.; Jackson, M. T.; Sampson, J. Dispersal and accumulation of Pt,
578 Pd and Rh derived from a roundabout in Sheffield (UK): From stream to tidal
579 estuary. *Sci. Total Environ.* **2008**, *401* (1), 90–99.

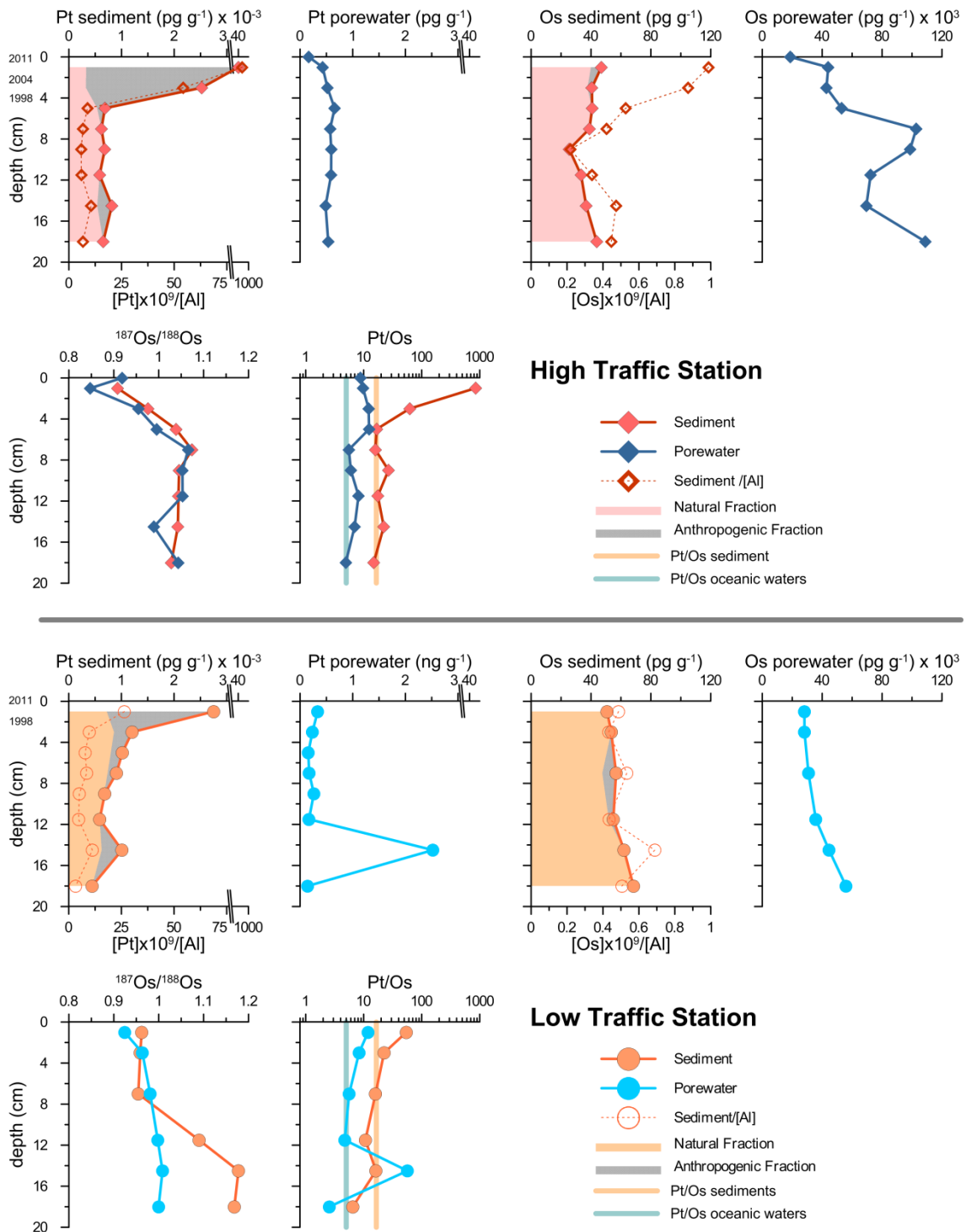
- 580 (51) Zereini, F.; Skerstupp, B.; Rankenburg, K.; Dirksen, F.; Beyer, J.-M.; Claus, T.;
581 Urban, H. Anthropogenic emission of platinum-group elements into the
582 environment. *J. Soils Sediments* **2001**, *1* (1), 44–49.
- 583 (52) Helmers, E.; Mergel, N. Platinum and rhodium in a polluted environment:
584 studying the emissions of automobile catalysts with emphasis on the application
585 of CSV rhodium analysis. *Fresenius J. Anal. Chem.* **1998**, *362* (6), 522–528.
- 586 (53) Mathur, R.; Ruiz, J.; Tornos, F. Age and sources of the ore at Tharsis and Rio
587 Tinto, Iberian Pyrite Belt, from Re-Os isotopes. *Miner. Deposita* **1999**, *34* (8),
588 790–793.
- 589 (54) Salgueiro, N.; Caçador, I. Short-term sedimentation in Tagus estuary, Portugal:
590 the influence of salt marsh plants. *Hydrobiologia* **2007**, *587* (1), 185–193.
- 591 (55) Schäfer, J.; Eckhardt, J.-D.; Berner, Z. A.; Stüben, D. Time-dependent increase of
592 traffic-emitted platinum-group elements (PGE) in different environmental
593 compartments. *Environ. Sci. Technol.* **1999**, *33* (18), 3166–3170.
- 594 (56) *Instituto Nacional de Estadística*. www.ine.es
- 595 (57) Poirier, A.; Gariépy, C. Isotopic signature and impact of car catalysts on the
596 anthropogenic osmium budget. *Environ. Sci. Technol.* **2005**, *39* (12), 4431–4434.
- 597 (58) Rodushkin, I.; Engström, E.; Sörlin, D.; Pontér, C.; Baxter, D. C. Osmium in
598 environmental samples from Northeast Sweden. Part II. Identification of
599 anthropogenic sources. *Sci. Total Environ.* **2007**, *386* (1), 159–168.
- 600 (59) Selby, D.; Creaser, R. A.; Fowler, M. G. Re–Os elemental and isotopic
601 systematics in crude oils. *Geochim. Cosmochim. Acta* **2007**, *71* (2), 378–386.
- 602 (60) McCandless, T. E.; Ruiz, J. Osmium isotopes and crustal sources for platinum-
603 group mineralization in the Bushveld Complex, South Africa. *Geology* **1991**, *19*
604 (12), 1225–1228.
- 605 (61) Walker, R. J.; Morgan, J. W.; Hanski, E. J.; Smolkin, V. F. Re-Os systematics of
606 early proterozoic ferropicrites, Pechenga Complex, northwestern Russia:
607 Evidence for ancient ¹⁸⁷Os-enriched plumes. *Geochim. Cosmochim. Acta* **1997**,
608 *61* (15), 3145–3160.
- 609 (62) Bruland, K. W.; Lohan, M. C. Controls of trace metals in seawater. *Oceans Mar.*
610 *Geochem.* Elderfield, H., Heinrich, D.H, Turekian, K.K. Eds.; Elsevier 2006, pp.
611 664.
- 612 (63) Turekian, K. K.; Sharma, M.; Gordon, G. W. The behavior of natural and
613 anthropogenic osmium in the Hudson River–Long Island Sound estuarine system.
614 *Geochim. Cosmochim. Acta* **2007**, *71* (17), 4135–4140.
- 615 (64) Chen, C.; Sedwick, P. N.; Sharma, M. Anthropogenic osmium in rain and snow
616 reveals global-scale atmospheric contamination. *Proc. Natl. Acad. Sci.* **2009**, *106*
617 (19), 7724–7728.
- 618 (65) McLennan, S. M. Relationships between the trace element composition of
619 sedimentary rocks and upper continental crust. *Geochem. Geophys. Geosystems*
620 **2001**, *2*, 1021.
- 621



622

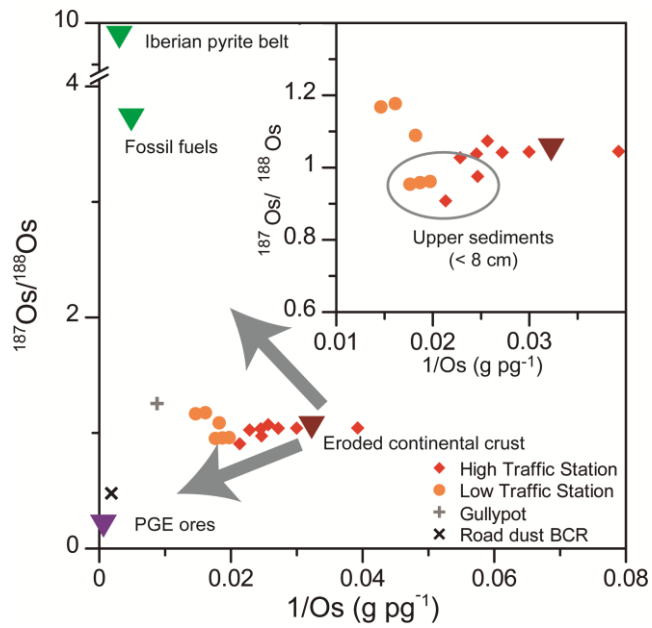
623

624 Figure 1: Map of study area location in the south bank of the Tagus Estuary (A: High
 625 Traffic Station, B: Low Traffic Station).



626

627 Figure 2: Pt concentration in sediment and porewater (pg g^{-1}) -concentrations
 628 normalized by Al in dashed lines-, Os concentration in sediment and porewater (pg g^{-1}),
 629 $^{187}\text{Os}/^{188}\text{Os}$ ratio and Pt/Os ratios. Natural and anthropogenic contributions for Pt and
 630 Os in sediments are shown as different areas in the total concentration. Mean Pt/Os
 631 ratios in oceanic waters (North Atlantic^{35,38}) and sediment¹ are indicated as vertical lines
 632 in Pt/Os, blue and orange, respectively.



633

634 Figure 3: $^{187}\text{Os}/^{188}\text{Os}$ vs. $1/[\text{Os}]_{\text{total}}$ (g pg^{-1}) in High Traffic Station and Low Traffic
 635 Station sediments, bridge gullypot and road dust reference material for this study. Fossil
 636 fuels^{58,59}, Iberian pyrite belt⁵³, PGE ores^{20,60,61} and eroded continental crust¹ define the
 637 potential Os sources. The plot shows two tendencies of anthropogenic impact (grey
 638 arrows).

639

Table 1: Blanks, detection limits (blank + 3xSD) and reference materials for the study: BCR-723 road dust reference material³⁷, PACS-2 marine sediment reference material⁴⁵.

Sediment sample	Pt (pg g ⁻¹)	Os (pg g ⁻¹)	¹⁸⁷ Os/ ¹⁸⁸ Os	Al (%)
Blank	24 ± 4 (n=10)	0.19 ± 0.07 (n=2)	0.288 ± 0.003 (n=2)	0.0004 ± 0.0001
DL	37	0.40	-	0.0007
BCR-723 (road dust)	81500 ± 6300 (n=7)	457	0.53	-
	(cert. 81300 ± 2500)	(cert. 460 ± 20)*	0.43	-
PACS-2 (marine sediment)	-	-	-	6.78 ± 0.75 (n=4) (cert. 6.63 ± 0.32)
Porewater sample	Pt (pg g ⁻¹)	Os (pg g ⁻¹)	¹⁸⁷ Os/ ¹⁸⁸ Os	
Blank	0.003 ± 0.003 (n=13)	0.0013 ± 0.0006 (n=2)	0.368 ± 0.044 (n=2)	-
DL (porewater)	0.013	0.0031	-	-

Values: mean value ± SD; number of replicates in brackets.

Sediment blanks for typical sediment mass of 200 and 500 mg for Pt and Os respectively.

Interstitial water blanks for 2 and 40 mL of sample for Pt and Os respectively.

*No certify value of Os in IRMM, value from Meisel et al. 2003⁴³.

Table 2: Sediment sample values of Al₂O₃ (% weight), Pt and Os concentrations (pg g⁻¹) and ¹⁸⁷Os/¹⁸⁸Os used for calculations of anthropogenic fraction for Pt and Os, in sediments of High Traffic Station core and gullypot, Low Traffic Station core, road dust reference material BCR-723, eroded continental crust^{1,65}, range of oceanic waters⁵¹ and water from North Atlantic^{35,38,64}. Anthropogenic fractions for Os (*AF_{Os}*) are calculated by Rauch et al. 2004 and 2006^{23,25} method (using isotopic rates) and anthropogenic fractions for Pt (*AF_{Pt}*) normalizing with Pt/Al ratios of background (normalization by Pt/Os ratios of eroded continental crust values (Rauch's method^{23,25}) or Pt/Os ratios of local background were calculated did not show important differences).

sample	Season	Depth (cm)	Al ₂ O ₃ (%)	[Pt] pg g ⁻¹	EF _{Pt}	AF _{Pt} (%)	[Os] pg g ⁻¹	EF _{Os}	¹⁸⁷ Os/ ¹⁸⁸ Os	AF _{Os} (%)	Pt/Os
High Traffic 0-2	Summer	0-2	9.0	40100	119	99	46.9	2.6	0.908	15	854
High Traffic 2-4		2-4	8.8	2520	7.6	87	40.6	2.3	0.976	7	62
High Traffic 4-6		4-6	14.6	683	1.2	19	40.8	1.4	1.038	0	17
High Traffic background		6-20	18.3 ± 2.6 ¹	670 ± 89 ¹	1.0 ± 0.3 ¹	6 ± 14 ¹	35.7 ± 6.8 ¹	1.0 ± 0.3 ¹	1.047 ± 0.008 ¹	0 ± 0 ¹	19 ± 5 ¹
Low Traffic 0-2	Spring	0-2	19.7	2750	4	77	50.7	0.9	0.962	18	54
Low Traffic 2-4		2-4	23.4	1200	1.6	38	53.5	0.8	0.959	19	22
Low Traffic 6-8		6-8	24.7	906	1.4	29	56.7	1.0	0.954	19	16
Low Traffic background		8-20	23.1 ± 4.1 ²	682 ± 240 ²	1.1 ± 0.7 ²	15 ± 27 ²	61.8 ± 6.7 ³	1.0 ± 0.2 ³	1.145 ± 0.048 ³	2 ± 3 ³	11 ± 5 ³
High Traffic Gullypot	-	-	18.3	157000	256	100	114	3	1.257	-	1380
Road Dust ref BCR-723	-	-	-	81500 ± 6300	160	99	457, 635	15, 21	0.531, 0.429	58, 69	128, 178
Eroded continental crust	-	-	15.2	510	-	-	31	-	1.05 ± 0.23	-	16
Oceanic waters	-	-	-	0.04-0.3	-	-	0.003-0.011	-	0.95	-	-
North Atlantic waters	-	-	-	0.05	-	-	0.010	-	1.05	-	5

Values: mean value ± SD Number of replicates¹n=5; ²n=4; ³n=3